Ab initio and DFT computational studies on molecular conformations and strength of the intramolecular hydrogen bond in different conformers of 3-amino-2-iminomethyl acryl aldehyde

6 AUTHORS, INCLUDING:

Mehdi Yoosefian
Kerman Graduate University of Technology
42 PUBLICATIONS **284** CITATIONS

SEE PROFILE

Fariba Mollania
University of Birjand
24 PUBLICATIONS **101** CITATIONS

SEE PROFILE

Alireza Nowroozi
University of Sistan and Baluchestan
37 PUBLICATIONS **311** CITATIONS

SEE PROFILE

Ab initio and DFT computational studies on molecular conformations and strength of the intramolecular hydrogen bond in different conformers of 3-amino-2-iminomethyl acryl aldehyde

Heidar Raissi [a], Mehdi Yoosefian [a,*], Fariba Mollania [a], Farzaneh Farzad [a], Ali Reza Nowroozi [b], Danial loghmaninejad [a]

[a] Chemistry Department, University of Birjand, Birjand, Iran
[b] Chemistry Department, Sistan and Balouchestan University, Zahedan, Iran

ABSTRACT

The intramolecular hydrogen bonding in 3-amino 2-iminomethyl acryl aldehyde (AIA) has been studied by ab initio and DFT calculations. All possible conformers of the two tautomeric structures of the respective compound were fully optimized at HF, MP2 and B3LYP levels with 6-311++G** basis set. From 33 different obtained conformers, the most stable one was planar and could be stabilized by the intramolecular N—H···N hydrogen bonding. In addition, harmonic vibrational frequencies were evaluated at the same levels to confirm the nature of the stationary points found and also to account for the zero point vibrational energy (ZPVE) correction. Furthermore the topological properties of the electron density distributions for N—H···N and N—H···O intramolecular hydrogen bond bridges were analyzed in terms of the Bader theory of atoms in molecules (AIM). The electron density (ρ) and Laplacian ($\nabla^2\rho$) properties, estimated by AIM calculations, indicate that N···H and O···H bond possess low ρ and positive ($\nabla^2\rho$) values and are in agreement with electrostatic character of the HBs, whereas N—H bonds have covalent character ($\nabla^2\rho < 0$). The theoretical calculations for AIA conformers in water solution were also carried out at B3LYP/6-311++G** level of theory. Our data indicate that the order of stability of AIA conformers is similar to their stability order in the gas phase.

© 2011 Elsevier B.V. All rights reserved.

1. Introduction

The prediction of the properties of intra and intermolecular hydrogen bonding is one of the most important concerns in science [1]. Similar to intermolecular hydrogen bonds, intramolecular hydrogen bondings also exist in numerous organic compounds and biomolecules, such as hormones, coenzymes and proteins. Such H-bonds play a significant role in biological phenomena, chemical reactions and formation of crystalline units which could lead to some kinds of structural distortions in many molecules from water to DNA. Several intermolecular hydrogen bondings have been observed in biological systems, such as OHO, NHO and NHN. Traditionally one of the most essential structures, capable of bearing hydrogen bond, is OHO unit, which has been studied extensively, but NHO and NHN units are the most frequent hydrogen bridges that exist in biological systems. Therefore both require further studies. Most frequently, H-bonds are from the X—H···Y type, where X and Y are electronegative elements (like F, O, and N) and Y possesses at least one electron lone pair. It is well known that the geometrical parameters of the HB reflect the strength of this bond. Also it is clear that the X—H proton donating bond due to the H-bond formation is usually elongated. This lengthening is greater for stronger H-bonds and could be measured for homogenous samples of complexes [2]. Y is an acceptor center. Usually, the shorter the H···Y distance, the stronger is the HB. The interaction energy values span from a typical van der Waals to a covalent interaction, usually between 2 and 10 kcal mol^{-1}. The H···Y distance should be smaller than the corresponding sum of the van der Waals radii of these atoms in order to have a pronounced interaction. Gilli et al. have proposed the RAHB model in order to link the strength of the hydrogen bonding to the resonance in chelated systems [7–11]. Many authors [12–16] have devised various methods to estimate the energy of intramolecular hydrogen bonding. Up to know attempts to calculate this value in the same way as intermolecular H-bonds have been failed.

An interesting representative compound that incorporates itself in a symmetric N—H···N classification of intramolecular hydrogen bonds is 3-amino 2-iminomethyl acryl aldehyde (AIA). AIA possesses the imine–amine equilibrium that shown in Fig. 1. In this equilibration, there are 8 and 7 possible amine and imine forms, respectively, capable of forming intramolecular hydrogen bonding.

* Corresponding author. Tel.: +98 5612502064; fax: +98 5612502065.
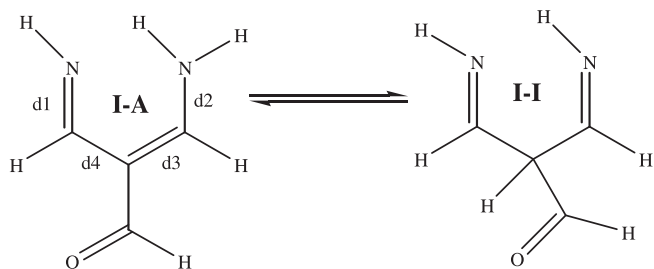 *E-mail address:* myoosefian@yahoo.com (M. Yoosefian).

Fig. 1. Tautomery equilibrium in AIA.

In this research we intend to determine the order of stability of the various conformations of AIA accompanying the theoretical evaluation in the gas phase and in water solution, and to compute the energies of the various hydrogen bridges present in the two tautomers. The outcome of these energy calculations is vital both for rationalizing the conformational equilibrium and for better understanding of the interactions governing the hydrogen bridge formation in the gas phase as well as in water.

2. Computational methods

In the present study, all the computations have been performed using the Gaussian 98 suite of programs [3]. To conduct the geometry optimization HF, MP2 and B3LYP methods with 6-311++G** basis set were employed. To define the nature of the acquired stationary points and to account for the zero point vibrational energy (ZPVE) corrections, harmonic vibrational frequencies were computed at the same levels of theory. All respective systems were fully optimized. Analysis of the electronic charge density (ρ) and its Laplacian ($\nabla^2\rho$) are accomplished by means of the theory of molecular structure proposed by Bader and coworker [4]. The calculated electron density, ρ, and its second derivative, $\nabla^2\rho$ were used for describing the nature of the intramolecular N—H···N and N—H···O hydrogen bonds. The AIM 2000 program was used to find and analyze the BCPs [5]. Finally, for a better understanding of the intramolecular interactions, the natural bond orbital (NBO) [6] analysis were carried out.

3. Results and discussion

3.1. Hydrogen bond

The extra stability of chelated forms of AIA is mainly due to the formation of intramolecular hydrogen bonding, assisted by π-electron delocalization (RAHB). Abromov has utilized Bader theory to evaluate the local kinetic energy density, $G(r)$, in terms of electron density $\rho(r)$, its gradient $\rho(r)$ and its Laplacian $^2\rho(r)$ functions [22]. At the critical points, where $\rho(r)=0$, the Abromov relation takes the form of:

$$G(r_{CP}) = (3/10)(3\pi^2)^{2/3}\rho^{5/3}(r_{CP}) + (1/6)\nabla^2\rho(r_{CP})$$

All the parameters in the above equation are expressed in atomic units. The local potential energy density $V(r_{CP})$ can be derived from the virial equation [22]:

$$2G(r_{CP}) + V(r_{CP}) = (1/4)\nabla^2\rho(r_{CP})$$

The simple relationship between H-bond energy and the potential energy density $V(r_{CP})$ at the critical point corresponding to N···H and O···H contacts was assigned to be $E_{HB} = 1/2\,V(r_{CP})$. We implemented this method to estimate H-bond energies (E_{HB}) for N···H and O···H contacts in AIA conformers, the results are listed in Tables 1 and 2. For the conformers studied here, the stronger is H-bond, the greater will be the elongation of the proton donating bond and the shorter is H···Y contact.

3.2. Molecular conformation

On the basis of the definition of the standard conformer, theoretically, AIA has thirty-three different plausible conformers, systematically arranged in two tautomeric classes, imine–amine (I–A) and imine–imine (I–I). Each one consists of 16 and 17 rotomers, respectively. The structures of all of these conformers are shown in Figs. 2 and 3. The relative energies of the stable forms at all of computational levels (B3LYP, MP2 and HF) are collected in Tables 3 and 4. Comparison of all hydrogen bonded and non-hydrogen bonded systems in all of conformers using mean energies provides the following stability order for AIA conformers at B3LYP/6-311++G** level (The values in parentheses refer to calculations at MP2/6-311++G** level and the values in brackets refer to calculations at HF/6-311++G** level).

H-bonded :	I–A	I–I
ΔE(kJ mol^{-1}) :	20.19(22.74)[19.63]	118.90(94.43)[94.04]

Non-H-bonded :	I–A	I–I
ΔE(kJ mol^{-1}) :	57.42(59.56)[49.46]	131.43(106.27)[101.62]

It can be concluded that the energy order in all of non-hydrogen bonded and hydrogen bonded systems are independent of both computational level and correlation energy. These energy differ-

Table 1
The geometrical parameters (r is in Å) and the energy of the intramolecular hydrogen bond (kJ mol^{-1}) for I–A conformers calculated at the B3LYP/6-311++G** level (values in parenthesis refer to calculations in water solution).

	C=N	C—N	C=C	C—C	N—H	C=O	Q	E_{HB}
I–A$_1$	1.291 (1.286)	1.329 (1.324)	1.385 (1.391)	1.444 (1.449)	1.026 (1.029)	1.219 (1.227)	0.0972	−36.23 (−39.61)
I–A$_2$	1.282 (1.281)	1.348 (1.338)	1.371 (1.378)	1.465 (1.464)	1.009 (1.009)	1.218 (1.22)	0.1596	–
I–A$_3$	1.289 (1.287)	1.334 (1.326)	1.380 (1.389)	1.452 (1.451)	1.025 (1.024)	1.218 (1.227)	0.1158	−35.68 (−34.26)
I–A$_4$	1.280 (1.281)	1.353 (1.339)	1.367 (1.377)	1.473 (1.469)	1.009 (1.009)	1.215 (1.223)	0.1795	–
I–A$_5$	1.279 (1.279)	1.331 (1.329)	1.385 (1.387)	1.461 (1.461)	1.019 (1.018)	1.234 (1.234)	0.1271	−32.02 (−30.08)
I–A$_6$	1.279 (1.281)	1.347 (1.336)	1.373 (1.383)	1.471 (1.465)	1.007 (1.008)	1.219 (1.227)	0.1666	–
I–A$_7$	1.278 (1.279)	1.334 (1.328)	1.382 (1.388)	1.470 (1.466)	1.019 (1.019)	1.232 (1.231)	0.1444	−34.52 (−31.20)
I–A$_8$	1.276 (1.279)	1.349 (1.335)	1.369 (1.381)	1.480 (1.472)	1.006 (1.008)	1.215 (1.223)	0.1851	–
I–A$_9$	1.277 (1.282)	1.335 (1.328)	1.382 (1.389)	1.469 (1.465)	1.018 (1.017)	1.231 (1.231)	0.1454	−32.36 (−28.77)
I–A$_{10}$	1.272 (1.282)	1.350 (1.332)	1.373 (1.39)	1.477 (1.469)	1.005 (1.009)	1.219 (1.23)	0.1825	−17.29 (−21.31)
I–A$_{11}$	1.276 (1.283)	1.352 (1.334)	1.370 (1.388)	1.464 (1.459)	1.006 (1.008)	1.208 (1.221)	0.1693	–
I–A$_{12}$	1.280 (1.284)	1.349 (1.334)	1.369 (1.382)	1.457 (1.459)	1.007 (1.009)	1.219 (1.229)	0.1569	–
I–A$_{13}$	1.274 (1.287)	1.352 (1.329)	1.373 (1.396)	1.469 (1.459)	1.006 (1.008)	1.209 (1.224)	0.1739	–
I–A$_{14}$	1.279 (1.283)	1.338 (1.331)	1.379 (1.386)	1.459 (1.458)	1.018 (1.016)	1.232 (1.235)	0.1394	−32.47 (−27.53)
I–A$_{15}$	1.278 (1.282)	1.346 (1.336)	1.371 (1.379)	1.466 (1.465)	1.007 (1.008)	1.219 (1.222)	0.1626	–
I–A$_{16}$	1.274 (1.28)	1.348 (1.334)	1.371 (1.385)	1.472 (1.468)	1.005 (1.008)	1.218 (1.229)	0.1751	−18.30 (−21.48)

Table 2
The geometrical parameters (r is in Å) and the energy of the intramolecular hydrogen bond (in kJ mol^{-1}) for I–I conformers calculated at the B3LYP/6-311++G** level (values in parenthesis refer to calculations in water solution).

	C=N	C—C	C—C	C=N	C—C	C=O	E_{HB}
I–I$_1$	1.264 (1.269)	1.518 (1.514)	1.514 (1.513)	1.265 (1.267)	1.535 (1.526)	1.202 (1.206)	–
I–I$_2$	1.260 (1.265)	1.545 (1.532)	1.507 (1.509)	1.271 (1.269)	1.521 (1.534)	1.204 (1.203)	−16.61 (−23.73)
I–I$_3$	1.267 (1.267)	1.513 (1.512)	1.524 (1.524)	1.265 (1.265)	1.535 (1.535)	1.201 (1.201)	−21.49 (−22.35)
I–I$_4$	1.271 (1.269)	1.507 (1.509)	1.545 (1.532)	1.260 (1.264)	1.521 (1.533)	1.204 (1.203)	−16.50 (−23.63)
I–I$_5$	1.266 (1.266)	1.525 (1.527)	1.520 (1.544)	1.267 (1.264)	1.539 (1.528)	1.201 (1.208)	–
I–I$_6$	1.258 (1.262)	1.556 (1.541)	1.503 (1.510)	1.270 (1.269)	1.521 (1.527)	1.204 (1.205)	−14.05 (−20.23)
I–I$_7$	1.266 (1.266)	1.514 (1.525)	1.542 (1.523)	1.263 (1.269)	1.525 (1.525)	1.206 (1.208)	−15.14 (−21.03)
I–I$_8$	1.267 (1.266)	1.517 (1.519)	1.511 (1.506)	1.268 (1.269)	1.546 (1.529)	1.196 (1.204)	–
I–I$_9$	1.267 (1.267)	1.512 (1.513)	1.524 (1.523)	1.267 (1.268)	1.534 (1.535)	1.203 (1.203)	–
I–I$_{10}$	1.268 (1.267)	1.509 (1.511)	1.515 (1.517)	1.269 (1.269)	1.537 (1.536)	1.203 (1.204)	–
I–I$_{11}$	1.264 (1.264)	1.529 (1.544)	1.517 (1.527)	1.266 (1.266)	1.538 (1.528)	1.199 (1.208)	–
I–I$_{12}$	1.266 (1.266)	1.533 (1.252)	1.512 (1.516)	1.266 (1.268)	1.536 (1.537)	1.197 (1.204)	–
I–I$_{13}$	0.267 (1.263)	1.520 (1.539)	1.514 (1.509)	1.269 (1.268)	1.543 (1.519)	1.201 (1.206)	–
I–I$_{14}$	1.267 (1.267)	1.526 (1.529)	1.523 (1.525)	1.267 (1.266)	1.531 (1.529)	1.203 (1.205)	–
I–I$_{15}$	1.264 (1.262)	1.531 (1.546)	1.531 (1.546)	1.266 (1.262)	1.519 (1.507)	1.206 (1.213)	−18.15 (−12.86)
I–I$_{16}$	1.267 (1.263)	1.529 (1.540)	1.515 (1.524)	1.266 (1.265)	1.548 (1.515)	1.197 (1.209)	–
I–I$_{17}$	1.263 (1.267)	1.532 (1.528)	1.516 (1.521)	1.267 (1.267)	1.524 (1.523)	1.206 (1.210)	−19.37 (−21.05)
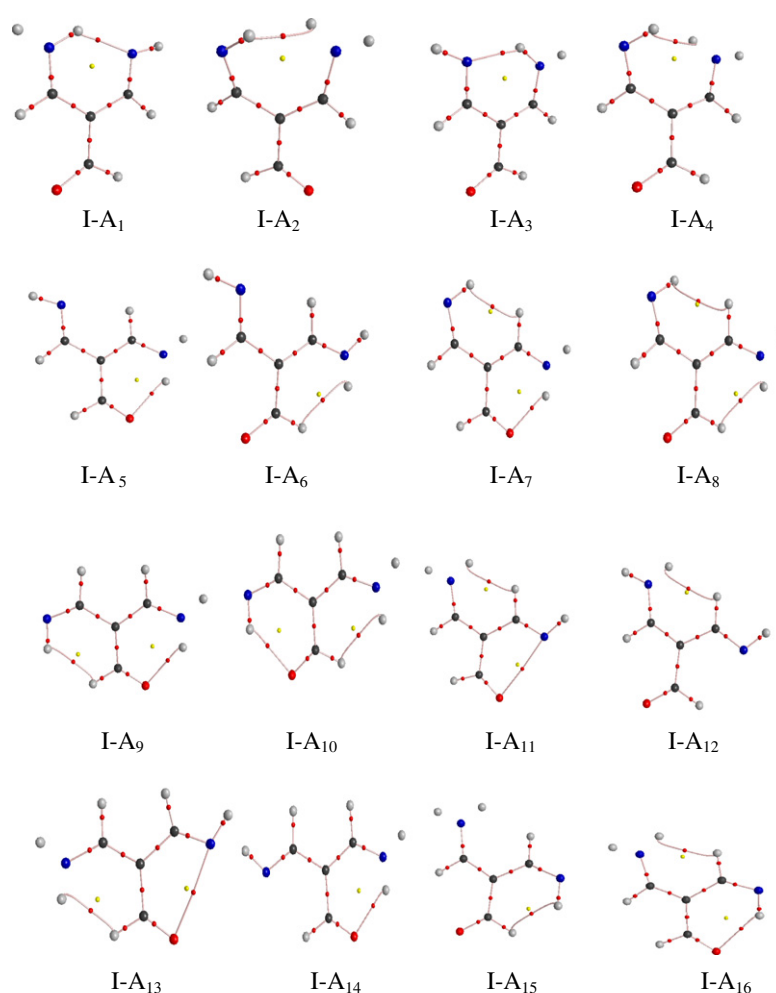
Fig. 2. Possible Imin–amin conformers in I–A.

ences are very important since their values represent the stabilization energy of imine–amine with respect to imine–imine in the presence or absence of HB. Furthermore, a ZPVE correction would not change the energy orders, being an insensitive parameter. The extra stability of imine–amine conformers is a wonderful phenomenon, confirmed by the various theoretical studies [23,24]. In some of the previous works, the greater stability of a imine–amine tautomer was solely attributed to the intramolecular hydrogen bond strength [25]. Our theoretical calculations showed that the hydrogen bond energies are not a major factor in determining of the preferred conformations. Although, in most amino compounds, the NH$_2$ functional group has the pyramidal shape, it is completely
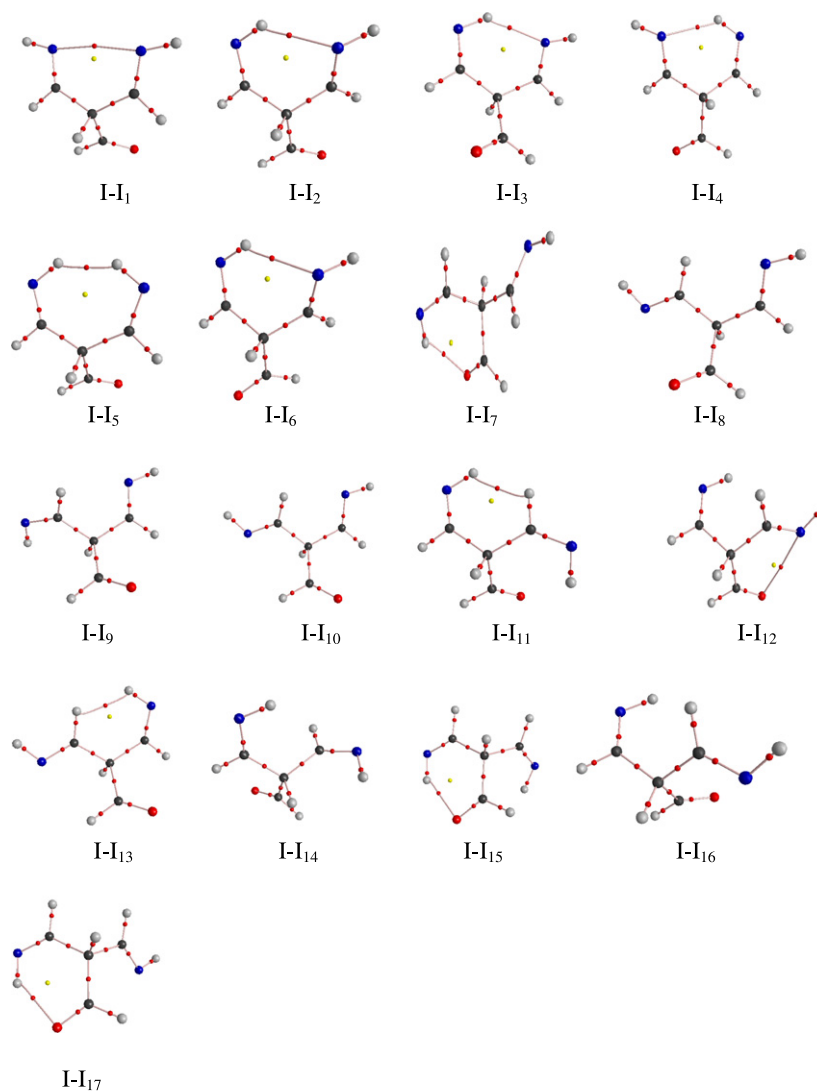
Fig. 3. Possible Imin–imin conformers in I–I.

Table 3
Stability order (S. O.) and relative energies (R. E.) of Imin–Amin conformers at various computational methods (kJ mol^{-1}).

B3LYP		MP2		HF	
S. O.	R. E	S. O.	R. E	S. O.	R. E
I–A$_3$	0.00	I–A$_3$	0.00	I–A$_3$	0.00
I–A$_1$	1.89	I–A$_1$	6.99	I–A$_1$	3.19
I–A$_5$	7.92	I–A$_5$	12.97	I–A$_5$	9.03
I–A$_{14}$	14.49	I–A$_{14}$	15.58	I–A$_{14}$	11.23
I–A$_9$	23.91	I–A$_9$	26.35	I–A$_9$	24.69
I–A$_7$	25.67	I–A$_7$	32.87	I–A$_7$	28.69
I–A$_{16}$	39.35	I–A$_{16}$	38.58	I–A$_6$	31.96
I–A$_6$	39.87	I–A$_6$	42.35	I–A$_{12}$	32.04
I–A$_{12}$	41.06	I–A$_{12}$	43.41	I–A$_{16}$	35.43
I–A$_{10}$	48.36	I–A$_4$	47.18	I–A$_4$	41.89
I–A$_{15}$	48.64	I–A$_{10}$	48.58	I–A$_{15}$	42.63
I–A$_2$	50.45	I–A$_2$	51.93	I–A$_2$	44.44
I–A$_4$	59.16	I–A$_{15}$	53.42	I–A$_{10}$	44.74
I–A$_{11}$	63.28	I–A$_{11}$	63.46	I–A$_{11}$	60.18
I–A$_{13}$	68.91	I–A$_{13}$	67.14	I–A$_{13}$	65.87
I–A$_8$	87.48	I–A$_8$	107.59	I–A$_8$	76.68

Table 4
Stability order (S. O.) and relative energies (R. E.) of Imin–Imin conformers at various computational methods (in kJ mol^{-1}).

B3LYP		MP2		HF	
S. O.	R. E	S. O.	R. E	S. O.	R. E
I–I$_4$	112.83	I–I$_3$	77.94	I–I$_{10}$	70.03
I–I$_2$	112.83	I–I$_9$	81.39	I–I$_9$	84.19
I–I$_9$	115.91	I–I$_{10}$	81.70	I–I$_2$	88.23
I–I$_6$	116.24	I–I$_6$	90.16	I–I$_4$	88.24
I–I$_7$	118.01	I–I$_{17}$	93.49	I–I$_{17}$	88.98
I–I$_{17}$	119.08	I–I$_2$	95.44	I–I$_{13}$	94.27
I–I$_{13}$	122.68	I–I$_4$	95.44	I–I$_8$	94.64
I–I$_3$	122.79	I–I$_8$	99.28	I–I$_7$	95.15
I–I$_8$	123.50	I–I$_7$	99.94	I–I$_{14}$	95.99
I–I$_{10}$	124.14	I–I$_{14}$	101.66	I–I$_6$	96.28
I–I$_{14}$	124.59	I–I$_{13}$	102.71	I–I$_3$	96.64
I–I$_{15}$	130.51	I–I$_{16}$	108.39	I–I$_{15}$	104.75
I–I$_{16}$	133.45	I–I$_{15}$	108.63	I–I$_{16}$	107.37
I–I$_{11}$	135.28	I–I$_{11}$	114.59	I–I$_{11}$	111.79
I–I$_{12}$	142.91	I–I$_{12}$	119.65	I–I$_1$	115.07
I–I$_1$	143.59	I–I$_1$	122.47	I–I$_{12}$	117.14
I–I$_5$	148.26	I–I$_5$	130.87	I–I$_5$	125.69

planar in all of I–A conformers, lying in the molecular plane. It means, the planar configuration of NH$_2$ functional group is imparted the greater stability to I–A conformers. This extra stability

of I–A conformers is mainly due to the participation of nitrogen lone pair in the π-electron resonance, not because of the π-conju-

gation of double bonds in I–A skeleton [26]. In I–A conformers the lone pair of nitrogen atom (with P character) is perpendicular to its molecular plane and participates completely in the π-electron resonance.

Unstability of I–I conformers is owing to the removal of two conjugated double bonds, giving rise to appearance of HC(COH). Among seventeen conformers of the imine–imine tautomer, there are four conformers possessing N—H···N H-bonds and three conformers having N—H···O H-bonds. By examining these conformers we were able to compare their H-bonds strength.

3.3. Imine–amine group

Structural parameters and the energy of the intramolecular hydrogen bondings are listed in Table 1. All the different conformers of I–A group are shown in Fig. 2. Because of π-electron conjugations, all imine–amine conformers can exhibit planar structures and are fully optimized, except for the I–A$_{11}$ conformer, which was forced to planarity. The I–A tautomers are quite interesting, since they show two types of intramolecular hydrogen bondings, i.e. N—H···N (I–A$_1$ and I–A$_3$) and N—H···O (I–A$_5$, I–A$_7$, I–A$_9$, I–A$_{10}$, I–A$_{14}$ and I–A$_{16}$). In the case of N—H···N hydrogen bonding, it is accompanied by the lengthening of N—H bond and shortening of N···N distance and in the case of N—H···O bond, the lengthening of N—H bond and shortening of N···O distance would occur. The values of calculated geometrical parameters indicate stronger N—H···N interactions with respect to N—H···O bonds. Namely, H···N distances within N—H···N hydrogen bonds are regularly shorter than H···O bonds. The comparison of the relative energies between different I–A conformers at all of the computational levels showed that in the most stable (I–A$_3$, I–A$_1$) and the least stable (I–A$_{13}$, I–A$_8$) conformeric pairs, stability energy difference is significant (see Table 3).

As it is obvious from Table 3, I–A$_3$ conformer is more stable than I–A$_1$. In both conformers, a relatively strong N—H···N intramolecular hydrogen bonding exists, and that the intramolecular hydrogen bonding in the cis (I–A$_1$) conformer is stronger than the trans one (I–A$_3$). However, their relative stability energies reveal that the trans orientation of the N—H and C=C bonds is more stable than cis orientation.

Regarding to the our theoretical results the hydrogen bonding in I–A$_7$ conformer is stronger than the others and this fact could be confirmed by comparison of the O···H distances in these conformers (see Table 1).

The resonance of π-electrons in the I–A conformers is another factor that strongly affects the stability of conformers, it produces by the hydrogen atom of NH group and a free electron pair of imine group. In the I–A$_1$ conformer, C=C, C=N and N—H bond lengths have been risen, whereas C—C and C—N bond lengths are reducing. Also electronic densities at C=C and C=N and N—H bond critical points are decreased, but the electronic densities at C—C and C—N bond critical points are enhanced with respect to other imine–amine conformers. These behaviors are caused by hydrogen bond formation, which in fact increases the π-electrons resonance in the chelated ring.

3.4. Imine–imine group

Here, seven conformers of imine–imine group are fully optimized while the other conformers, i.e. I–I$_1$, I–I$_3$, I–I$_5$, I–I$_7$, I–I$_8$, I–I$_{11}$, I–I$_{12}$, I–I$_{13}$, I–I$_{15}$, and I–I$_{16}$ represents non planar structures. For the sake of simplicity in comparing conformers structures, the planarity was imposed on them. The structurally possible imine–imine tautomeric conformers are shown in Fig. 3, mentioning that the geometrical parameters and hydrogen bond energy can be observed in Table 2. The results of theoretical calculations

on the stability orders of I–I conformers at all levels of theory (Table 4) illustrate that in spite of the presence of N—H···N and N—H···O hydrogen bondings, they are less stable than I–A conformers. In I–I$_2$, I–I$_3$, I–I$_4$ and I–I$_6$ conformers, the hydrogen of imine and lone pair of other imine functional group interact with each other and a new N—H···N hydrogen bond forms, while for I–I$_7$, I–I$_{15}$ and I–I$_{17}$ conformers, N—H···O hydrogen bondings exist.

Comparison of results presented in Tables 1 and 2 reveals that, the N—H···N intramolecular hydrogen bond energies theme in I–I conformers were considerably weaker than that in I–A conformers. Furthermore, the greater value of N···N distance in I–I$_2$, I–I$_3$, I–I$_4$ and I–I$_6$ against the I–A$_1$ and I–A$_3$ confirms the existence of weaker hydrogen bonding in I–I conformers. The same results observed for N—H···O intramolecular hydrogen bonding in I–I$_7$, I–I$_{15}$ and I–I$_{17}$ conformers. Geometrical parameters presented in Table 2 showed that the C=N, C—C, C—C, and C=N bond distances in I–I conformers were fairly similar and do not change noticeably even for the hydrogen bonded conformers. This means that the energy function was insensitive to the changes of bond distance.

3.5. AIM analysis

The "atoms in molecules" theory of Bader (AIM) [27] provides a solid foundation for the estimation of hydrogen bond energy [18–21]. The Bader theory is based on topological properties of the electron density (ρ_{BCP}), and Laplacian of the electron density ($^2\rho_{BCP}$) at the bond critical points (BCP) of two hydrogen bonded atoms. Therefore, the analysis of bond critical points was applied in order to obtain the hydrogen bond energy. It is well known that the hydrogen bond energy is related to (ρ) at the H···Y BCP and ($^2\rho$), of electron density at BCP of two hydrogen bonded atoms [28]. If a hydrogen bond exists, then the range of ρ_{BCP} and $^2\rho_{BCP}$ are 0.002–0.035 and 0.024–0.139 a.u., respectively. The atomic interactions may be classified in two general classes, shared interactions and closed-shell interactions. The former (as covalent and polar bonds) is caused by a contraction of the charge density toward the line of interaction linking the nuclei. For this interaction the electronic charge is concentrated in the internuclear region and $\nabla^2\rho < 0$. The latter is governed by the contraction of the charge density toward each of interacting nuclei. In this case, the electronic charge is depleted in the interatomic surface and $\nabla^2\rho > 0$. The calculated electron density properties of I–A and I–I conformers showed that N···H and O···H bondings had low ρ_{BCP} and positive $\nabla^2\rho_{BCP}$ values (see Table 5). These properties are typical for closed-shell interactions as HBs and indicate electrostatic character of the N···H and O···H bondings [29]. The calculated Laplacian at the critical points for N—H bonds in I–A and I–I conformers have

Table 5
The topological parameters (in au) – the electron densities at H···X BCPs, for I–A and I–I conformers (values in parenthesis refer to calculations in water solution).

Conformer	X	$\rho_{(X···H)}$	$\nabla^2_{(X···H)}$
I–A$_1$	N	0.032579 (0.034825)	0.102136 (0.106192)
I–A$_3$	N	0.032215 (0.031269)	0.101424 (0.099318)
I–A$_5$	O	0.028907 (0.027674)	0.10504 (0.100527)
I–A$_7$	O	0.030468 (0.028378)	0.11076 (0.103271)
I–A$_9$	O	0.02902 (0.026727)	0.10692 (0.098324)
I–A$_{10}$	O	0.019016 (0.021941)	0.06468 (0.076302)
I–A$_{14}$	O	0.029164 (0.025999)	0.1064 (0.094451)
I–A$_{16}$	O	0.019817 (0.022123)	0.06732 (0.076239)
I–I$_2$	N	0.018835 (0.024027)	0.05998 (0.079071)
I–I$_3$	N	0.022323 (0.022956)	0.074504 (0.076517)
I–I$_4$	N	0.018746 (0.023951)	0.059656 (0.078887)
I–I$_6$	N	0.016746 (0.021584)	0.052916 (0.069604)
I–I$_7$	O	0.017324 (0.02159)	0.05848 (0.07687)
I–I$_{15}$	O	0.019532 (0.015438)	0.068256 (0.05162)
I–I$_{17}$	O	0.02047 (0.02166)	0.07152 (0.076458)

negative values, thus pointing out that N—H bonds in both conformers have covalent character.

In general, the strength and the length of the chemical bond are closely correlated. The bond strength is determined by accumulation of electron density in the bond region and the screening of nuclei by this density [30]. These characteristics of electron densities and its Laplacian at BCPs signify the presence of HB interaction. As shown in Table 5, comparison between the topological properties of I–A$_1$ and I–A$_3$ shows that these values for I–A$_1$ are slightly greater than the corresponding values of I–A$_3$. Consequently, the HB in I–A$_1$ is slightly stronger than the I–A$_3$. The same trend resurfaces in the all of conformers containing hydrogen bonding.

3.6. NBO Analysis

In the NBO analysis, the electronic wave functions are interpreted in terms of a set of occupied Lewis and a set of non-Lewis localized orbitals [31]. Delocalization effects can be identified from the presence of off diagonal elements of the Fock matrix. The strengths of these delocalization interactions, $E^{(2)}$, are estimated by second order perturbations theory.

The results of our NBO analysis (occupation number for the assignments and their orbital energies) for AIA conformers are provided in Table 6, demonstrating, the NBO occupation numbers for σ^*(N—H) antibonds, the nitrogen lone pair electrons (n_N) and their respective orbital energies (E). Furthermore, the donor–acceptor interactions and their second order perturbation stabilization energies $E^{(2)}$ (calculated at B3LYP/6-311++G** level of theory) for the chelated conformers of I–A and I–I are given in Table 6. As it is common, the orbital energies, ε, have been reported in a.u. while the second order perturbation energies $E^{(2)}$ are in kcal/mol. Moreover, the charge transfer between the lone pair electrons of the proton acceptor and antibonding of proton donors induce a significant interaction. The results of NBO analysis showed that in the chelated structures of the AIA conformers, two lone pair electrons of nitrogen and oxygen atoms (n_{2S}) participated as donor and σ^*(N—H) antibonding as acceptors. The strength of intramolecular hydrogen bond in AIA conformers was again supported by the NBO data. The HB charge transfer greatly changes the occupation number of nitrogen lone pairs and σ^*(N—H). The occupation numbers of σ^*(N—H) in non-HB conformers were remarkably small, whereas the corresponding value for nitrogen lone pairs was so close to the standard value of the 2. These values explicitly showed that no charge transfer between the lone pairs of nitrogen and σ^*(N—H) had occurred. Nonetheless, the corresponding values in chelated conformers were greatly changed. The occupation number of the σ^*(N—H) antibonding increased from I–A to I–I, and their orbital energies were also enhanced in the same manner. These results

can be rationalized in terms of the charge transfer interactions between orbitals. Our findings show that the charge transfer energy increases as follows: I–A$_1$, I–A$_3$, I–I$_6$, I–I$_4$, I–I$_2$ and I–I$_3$. Similar trend could be observed for all conformers containing the N—H···O intramolecular hydrogen bonding.

3.7. Resonance

Special attention has been often paid to strong intramolecular H-bonds and so-called resonance assisted hydrogen bonds (RAHBs). A quite number of RAHBs have been found among the crystal structures of β-diketone enols. For such systems the existence of π-electron delocalization of the O=C—C=C—OH keto-enol group have been proved. According to the statements of Gilli and co-workers [9] such π-electron delocalization is responsible for the changes in the geometry of the skeleton, filling the space between H-bond donor and acceptor. Nonetheless, the π-electron delocalization is inseparable from the other similar phenomenon, such as aromaticity. The effect of π-electron delocalization on the characteristic of RAHB has been also investigated [32–35]. The results of our work regarding π-electron delocalization within intramolecular RAHBs are: (i) the C—N and C—C bond lengths approach to C=N and C=C bond lengths, respectively; (ii) the N—H bond is lengthening while the H···N and N···N distances become shorter and the proton shifts towards the center of N···N contact.

The equalization of the mentioned bonds length for RAHB system is a consequence of direct geometry of the π-electron delocalization. A parameter of Q for such delocalization has been proposed as follows:

$$Q = (d2 - d1) + (d4 - d3)$$

Here, $d1$, $d2$, $d3$ and $d4$ are bond lengths (Fig. 1). The correlations of Q parameter with the other hydrogen bonding parameters have been examined showing the lowest value of Q, for the stronger H-bond and greater π-electron delocalization. The values of Q for the systems probed here are given in Table 1. As it is obvious from this table, the greatest value of Q has occurred for I–A$_8$ and the lowest value of Q was for I–A$_1$. Comparison of Q in I–A$_1$ and I–A$_3$ conformers shows that Q value in I–A$_1$ is lower than I–A$_3$. This fact confirms that the resonance in this conformer is more pronounced than the I–A$_3$.

The linear correlation coefficient was found to be 0.859 which shows dependency of Q on N—H bond length. Therefore, Q could be easily evaluated from N—H bond length, as follows:

$$Q = -3.158(r_{N-H}) + 3.351$$

3.8. The conformers in water solution

It is known that the hydrogen bond strength in solution is weaker when compared to the gas phase and its energy decreases when the dipole moment of the solvent increases. As a consequence, the conformational equilibrium could also undergo remarkable changes. To investigate the geometry and the intramolecular hydrogen bond energy changes in the various AIA conformers, B3LYP/6-311++G** optimization in water solutions were carried out. The solvent effect was calculated using the self-consistent reaction field (SCRF) model [36]. The geometrical and topological parameters of I–A and I–I conformers in water solution have been presented in Tables 1, 2 and 5. Our theoretical calculations showed that I–A conformers in water solution are more stable than gas phase. After optimization II$_1$, II$_5$, II$_{12}$, II$_{13}$ and II$_{16}$ convert to II$_{10}$, II$_{11}$, II$_6$, II$_6$ and II$_{17}$, respectively.

Comparison of all hydrogen bonded and non-hydrogen bonded systems in I–A and I–I conformers using mean energies revealed the following order of energetic stability (in the water phase):

Table 6
The NBO analysis data for I–A and I–I conformers at B3LYP/6-311++G** level of theory.

Conformer	LP → σ^*_{NH}	O. N$_{(LP)}$	O. N$_{\sigma^*(NH)}$	E$_{(LP)}$	E$_{\sigma^*(NH)}$
I–A$_1$	11.65	1.9215	0.0409	−0.41	0.4038
I–A$_3$	11.49	1.9252	0.0399	−0.4112	0.4049
I–A$_5$	6.53	1.8825	0.0303	−0.2801	0.4021
I–A$_7$	7.07	1.8819	0.0313	−0.2891	0.3946
I–A$_9$	6.27	1.8865	0.0288	−0.2911	0.3979
I–A$_{10}$	2.56	1.8797	0.0181	−0.278	0.4684
I–A$_{14}$	6.48	1.8909	0.0294	−0.2805	0.4059
I–A$_{16}$	2.89	1.8741	0.019	−0.2712	0.4623
I–I$_2$	2.24	1.9429	0.0219	−0.4271	0.4344
I–I$_3$	4.44	1.9349	0.0217	−0.4327	0.4605
I–I$_4$	2.21	1.9429	0.0218	−0.4271	0.4341
I–I$_6$	1.38	1.9128	0.0209	−0.3979	0.4294
I–I$_7$	1.47	1.8741	0.0188	−0.3077	0.4382
I–I$_{15}$	2.5	1.8786	0.015	−0.3172	0.3955
I–I$_{17}$	2.78	1.8803	0.0102	−0.301	0.4099

H-bonded :	I–A	I–I
$\Delta E(\text{kJ mol}^{-1})$	3.45	129.31
Non-H-bonded :	I–A	I–I
$\Delta E(\text{kJ mol}^{-1})$	36.01	125.41

In comparing the results we concluded that the order of stability of AIA conformers was similar to their stability order in the gas phase. Also, average energies comparison pointed out that, conformers containing hydrogen bonding in gas phase were more stable than the solution phase. The findings for non-hydrogen bonding systems were vice versa. The stability orders of I–A and I–I conformers are given in Table 7. The output of our theoretical calculations indicates that I–A_3 is the most stable conformer in both phases (water and gas). Intramolecular hydrogen bond energies of the I–A and I–I conformers have been calculated using the Espinosa method [17] and presented in Tables 1 and 2. Probe of these values depicted that hydrogen bonding strength of I–A_1 conformer in solution phase is stronger than gas phase but the N—H$\cdots$N hydrogen bonding for I–A_3 in gas phase is stronger than that of water solution. The comparison of N$\cdots$H distance in I–A_1 in gas phase and in water solution reaffirmed that N—H$\cdots$N bonding in water solution is stronger than that of gas phase. On the other hand, N—H$\cdots$O hydrogen bonding of I–A_7 in gas phase is stronger than that of solution phase. The comparison of O$\cdots$H distance in I–A_7 in gas phase and water solution demonstrates that N—H$\cdots$O bonding in gas phase is stronger than water solution. The results of Table 2 showed that the hydrogen bonding strength in I–I conformers in water solution is stronger than gas phase, but their stability orders in water and gas phase are different. Examination the total stability energy values in the solution and gas phase is interesting, because it points out that full optimization in a solvent is often not necessary, since only modest changes are noted with respect to the geometrical parameters obtained in the gas phase.

3.9. Conclusions

Hydrogen bonding strength was examined based on the geometric parameters obtained from ab initio or DFT calculations. Since the geometrical criteria for the existence of hydrogen bonding are controversial, the 'atoms in molecules' (AIM) theory was applied to analyze this type of interaction. To avoid ambiguity, our studies were restricted only to geometrical and topological parameters derived from the Bader's theory, population and NBO analysis. According to the all of theoretical calculations, the stability orders for the 3-amino 2-iminomethyl acryl aldehyde conformers in gas phase are:

I–A_3 < I–A_1 < I–A_5 < I–A_{14} < I–A_9 < I–A_7 < I–A_{16} < I–A_6

$< $ I–A_{12} < I–A_{10} < I–A_{15} < I–A_2 < I–A_4 < I–A_{11} < I–A_{13}

$< $ I–A_8 < I–I_4 < I–I_2 < I–I_9 < I–I_6 < I–I_7 < I–I_{17} < I–I_{13}

$< $ I–I_3 < I–I_8 < I–I_{10} < I–I_{14} < I–I_{15} < I–I_{16} < I–I_{11}

$< $ I–I_{12} < I–I_1 < I–I_5

Moreover, theoretical calculations indicate that the I–A_3 is the most stable conformer of AIA both in the gas phase and in water solution. The extra stability of I–A conformers could be attributed to π-electron delocalization of chelated ring induced by the H-bond formation. We concluded that in the gas phase, the hydrogen bond strength in I–I conformers (N—H$\cdots$N) is weaker than the water solution. Our findings also showed that ZPVE correction did not have any significant effect on stability order of these conformers. The N—H$\cdots$N bridge is the strongest hydrogen bonding which present in I–A_1 conformer.

References

[1] J. Emsley, Struct. Bonding (Berlin). 57 (1984) 147.
[2] S.J. Grabowski, Chem. Phys. Lett. 338 (2001) 361.
[3] M.J. Frisch, G.W. Trucks, H.B. Schlegel, G.E. Scuseria, M.A. Robb, J.R. Cheeseman, G. zakrzewski, J.A. Montgomery, R.E. Stratmann, J.C. Burant, S. Dapprich, J.M. Millam, A.D. Daniels, K.N. Kudin, M.C. Strain, O. Farkas, J. Tomasi, V. Barone, M. Cossi, R. Cammi, B. Mennucci, C. Pomelli, C. Adamo, S. Clifford, J. Ochterski, G.A. Petersson, P.Y. Ayala, Q. Cui, K. Morokuma, D.K. Malick, A.D. Rabuck, K. Raghavachari, J.B. Foresman, J. Cioslowski, J.V. Ortiz, B.B. Stefanov, G. Liu, A. Liashenko, P. Piskorz, I. Komaromi, R. Gomperts, L.R. Martin, D.J. Fox, T. Keith, M.A. Al-Laham, C.Y. Peng, A. Nanayakkara, G. Gonzalez, M. Challacombe, P.M.W. Gill, B. Johnson, W. Chen, M.W. Wong, J.L. Andres, C. Gonzalez, M. Head-Gordon, E.S. Replogle, J.A. Pople, GAUSSIAN98 Revision A. 6, Gaussian, Inc., Pittsburgh, PA, 1998.
[4] T. Steiner, E.B. Starikov, A.M. Amado, J.J.C. Teixera-Dias, J. Chem. Soc. Perkin 2 (1995) 1321.
[5] AIM2000 designed by Friedrick biegler – Konig, University of Applied Scievces, Bielefed, Germany.
[6] E.D. Glendening, A.E. Reed, J.E. Carpenter, F. Weinhold, NBO, Version 3.1, Gaussian, Inc., Pittsburgh, PA, 1992.
[7] G. Gilli, F. Bellucci, V. Ferretti, V. Bertolasi, J. Am. Chem. Soc. 111 (1989) 1023.
[8] V. Bertolasi, P. Gilli, V. Ferretti, G. Gilli, J. Am. Chem. Soc. 113 (1991) 4917.
[9] P. Gilli, V. Bertolasi, V. Ferretti, G. Gilli, J. Am. Chem. Soc. 116 (1994) 909.
[10] P. Gilli, V. Bertolasi, V. Ferretti, G. Gilli, J. Am. Chem. Soc. 122 (2000) 10405.
[11] P. Gilli, V. Bertolasi, L. Pretto, V. Ferretti, G. Gilli, J. Am. Chem. Soc. 126 (2004) 3845.
[12] P. Shuster, G. Zundel, The Hydrogen Bond, Recent Development in Theory and Experiment, North Holland, Amsterdam, 1976.
[13] I. Rozas, I. Alkorta, J. Elguero, J. Phys chem. A. 105 (2001) 10462.
[14] E. Espinosa, E. Molins, J. Chem. Phys. 113 (2000) 5686.
[15] A. Nowroozi, H. Raissi, F. Farzad, J. Mol. Struct. (THEOCHEM) 730 (2005) 161.
[16] M. Jablonski, A. Kaczmarek, A.J. Sadlej, J. Chem. Phys. A 110 (2006) 10890.
[17] E. Espinosa, E. Molins, C. Lecomte, Chem. Phys. Lett. 285 (1998) 170.
[18] M.T. Carroll, C. Chang, R.F.W. Bader, Mol. Phys. 63 (1988) 387.
[19] M.T. Carroll, R.F.W. Bader, Mol. Phys. 65 (1988) 695.
[20] U. Koch, P. Popelier, J. Chem. Phys. 99 (1995) 9747.
[21] O. Mo, M. Yanez, J. Elguero, J. Mol. Struct. (THEOCHEM) 314 (1994) 73.
[22] Y.A. Abromov, Acta Crystallogr. A 53 (1997) 264.
[23] H. Raissi, A.F. Jalbout, M.A. Nasseria, M. Yoosefian, H. Ghiassi, A.J. Hameed, Int. J. Quant. Chem. 108 (2008) 1444.
[24] H. Raissi, A.F. Jalbout, M. Fazli, M. Yoosefian, H. Ghiassi, Z. Wang, A.De. Leon, Int, J. Quant. Chem. 109 (2009) 1497.
[25] G. Buemi, F. Zuccarello, Electr. J. Theor. Chem. 2 (1997) 302.
[26] M. Fazli, A.F. Jalbout, H. Raissi, H. Ghiassi, M. Yoosefian, JTCC 8 (2009) 713.
[27] R.F.W. Bader, Atoms in Molecules a Quantum theory, Oxford University press, New York, 1990.
[28] S.J. Grabowski, J. Mol. Struct. 562 (2001) 137.
[29] R.F.W. Bader, ACC. Chem. Res. 18 (1985) 9.
[30] E. Kraka, D. Cremer, Chemical implication of local features of the electron density distribution in theoretical models of chemical bonding, in: Z.B. Maksic (Ed.), The Concept of Chemical Bond, vol. 2, Springer-Verlag, 1990.
[31] A.E. Reed, L.A. Curtis, F.A. Weinhold, Chem. Rev. 88 (1988) 899.
[32] P.V.R. Schleyer, Chem. Rev. 105 (2005) 3433.
[33] T.M. Krygowski, M.K. Cyranski, Chem. Rev. 101 (2001) 1385.
[34] S.J. Grabowski, J. Mol. Struct. (THEOCHEM). 811 (2007) 61.
[35] S.J. Grabowski, J. Phys. Org. Chem. 16 (2003) 797.
[36] L. Onsager, J. Am. Chem. Soc. 58 (1936) 1486.

Table 7
Stability order (S. O.) and relative energies (R. E.) of I–A and I–I conformers at B3LYP/6-311++G** level of theory in water solution (in kJ mol^{-1}).

Imin–Amin		Imin–Imin	
S. O.	R. E	S. O.	R. E
I–A_3	0.00	I–I_{17}	121.90
I–A_1	6.89	I–I_{10}	123.52
I–A_{14}	13.74	I–I_7	123.62
I–A_{10}	21.66	I–I_8	126.26
I–A_{16}	21.81	I–I_6	128.53
I–A_5	23.89	I–I_2	128.87
I–A_{12}	26.60	I–I_3	129.67
I–A_9	27.25	I–I_4	130.16
I–A_7	32.23	I–I_9	131.74
I–A_{13}	36.28	I–I_{14}	140.26
I–A_{11}	39.62		
I–A_6	41.26		
I–A_4	41.44		
I–A_{15}	50.81		
I–A_2	55.27		
I–A_8	72.23		